

## **OPTIMAL MICROSTRIP T-JUNCTIONS**

J.W. Bandler, M.A. Ismail and D.G. Swanson, Jr.

SOS-98-19-R

August 1998

© J.W. Bandler, M.A. Ismail and D.G. Swanson, Jr. 1998

No part of this document may be copied, translated, transcribed or entered in any form into any machine without written permission. Address inquiries in this regard to Dr. J.W. Bandler. Excerpts may be quoted for scholarly purposes with full acknowledgment of source. This document may not be lent or circulated without this title page and its original cover.

# OPTIMAL MICROSTRIP T-JUNCTIONS

J.W. Bandler, M.A. Ismail and D.G. Swanson, Jr.\*

Simulation Optimization Systems Research Laboratory  
and Department of Electrical and Computer Engineering  
McMaster University, Hamilton, Canada L8S 4L7

Tel 905 525 9140 Ext. 24305  
Fax 905 523 4407  
Email awad@soya.sos.mcmaster.ca

**Abstract** In this work, we compare different configurations to compensate discontinuities in a T-junction. The comparison is based on direct optimization of the different T-junction configurations in a broad frequency range. Four configurations are discussed here, three of them are mentioned in the literature and the other is introduced here. The T-junctions are optimized to achieve the possible minimum mismatch at the three ports. We believe that such comparison is helpful for microwave designers to choose the best configuration to compensate discontinuities in T-junctions.

## I. INTRODUCTION

In this report, we compare between four different configurations to compensate T-junction discontinuities. The T-junction discussed here is symmetric and is connected to three  $50 \Omega$  transmission lines. The first configuration is shown in Fig. 1(a) and was suggested in [1]. The discontinuity is compensated by removing a triangle portion from the basic T-junction as shown in Fig. 1(a). The T-junction configuration in Fig. 1(b) was introduced in [2] but no optimization was performed. In this case, the compensation for discontinuity is simply done by modifying the common arm and the two corners as shown in Fig. 1(b). The T-junction in Fig. 1(c) is introduced here and is similar to that in Fig. 1(b). The one in Fig. 1(d) is suggested in [3] but again no optimization was applied. The T-junction in Fig. 1(a) and (b) were compared in [4] but also no optimization was applied. The optimization variable for the T-junction in Fig. 1(a) is the side length  $r$  at  $\theta$  equal to  $30^\circ$ ,  $45^\circ$  and  $60^\circ$ . For the T-junctions in Fig. 1 (b),

---

This work was supported by the Natural Sciences and Engineering Research Council of Canada under Grants OGP0007239, STP0201832 and through the Micronet Network of Centers of Excellence.

\* D.G. Swanson is with M/A-COM, Inc. Corporate R&D, M/S 0L3, 100 Chelmsford Street, Lowell, MA 01853-3294.

(c) and (d) the optimization variables are  $x$  and  $y$ . These variables should be adjusted to satisfy the required specifications given in Section II.

## II. DESIGN SPECIFICATIONS

The four T-junction configurations in Fig. 1 are optimized to satisfy the theoretical simultaneous match condition which is 9.54 dB ( $20 \log (1/3)$ ) return loss at the three ports. In other words the specifications are

$$|S_{11}| \leq \frac{1}{3}, \quad |S_{22}| \leq \frac{1}{3}, \quad (1)$$

in the frequency range 2 GHz to 16 GHz. The width  $w$ , the height  $h$  and the relative dielectric constant  $\epsilon_r$  are fixed during optimization ( $w=24$  mil,  $h=25$  mil and  $\epsilon_r=9.9$ ). Three tools are utilized here to apply direct optimization, Sonnet's *em* simulator [5] to compute the scattering parameters of the different T-junction configurations, the minimax optimizer in OSA90/hope [6] to perform optimization and Empipe [6] to parameterize the geometry of the T-junctions.

## III. OPTIMIZATION RESULTS

The T-junction in Fig. 1(a) was optimized to satisfy the matching condition in (1). The side length  $r$  of the removed triangle with  $\mathbf{q}$  equal to  $30^\circ$ ,  $45^\circ$  and  $60^\circ$  is considered. The optimization has been carried out at each value of  $\mathbf{q}$  and the optimal values of  $r$  are given in Table I. Fig. 2 shows  $|S_{11}|$  and  $|S_{22}|$  at the optimal value of  $r$  for  $\mathbf{q} = 0^\circ$  (basic T-junction without any compensation),  $30^\circ$ ,  $45^\circ$  and  $60^\circ$ . It is clear that the responses at  $\mathbf{q} = 30^\circ$  have the least deviation from the ideal value of  $-9.54$  dB.

The T-junction in Fig. 1(b) was suggested in [2] to compensate discontinuity but no optimization was performed. This T-junction is optimized here with respect to  $x$  and  $y$  (shown in Fig. 1(b)) to satisfy (1). The optimization has been done from five starting points and reached a unique solution for  $x$  and  $y$ . The optimal values for  $x$  and  $y$  are given in Table II. Fig. 3(a) and (b) show  $|S_{11}|$  and  $|S_{22}|$  at the five starting points before and after optimization, respectively. It is clear from Fig. 3(b) that the response after optimization is very close to the required specifications in (1).

The compensation technique in Fig. 1(c) was not mentioned in the literature and is proposed here. The parameters  $x$  and  $y$  shown in Fig. 1(c) are optimized to satisfy the specifications in (1). The optimization was performed from five starting points and reached a unique value for  $x$  and  $y$  as given in Table II. Fig. 4(a) and (b) show  $|S_{11}|$  and  $|S_{22}|$  at the five starting points before and after optimization, respectively. It is clear from Fig. 4(b) that the response after optimization is fairly close to the required specifications in (1).

The T-junction configuration in Fig. 1(d) was suggested in [3]. It is optimized here with respect to  $x$  and  $y$  to satisfy (1). The optimization was performed from five starting points and reached one solution for  $x$  and  $y$  given in Table II. Fig. 5(a) and (b) show  $|S_{11}|$  and  $|S_{22}|$  at the five starting points before and after optimization, respectively. It is clear from Fig. 5(b) that the response after optimization is very close to the required specifications in (1).

Fig. 6 shows  $|S_{11}|$  and  $|S_{22}|$  in the frequency range 2 GHz to 20 GHz for the optimized T-junctions in Fig. 1. It is clear that the T-junction in Fig. 1(a) with  $q$  equal to  $30^\circ$  gives the worst results since  $|S_{11}|$  and  $|S_{22}|$  are very far from the ideal value of  $-9.54$  dB. The other T-junctions give satisfactory results with almost minor differences among their responses. Fig. 7 shows  $|S_{11}|$  and  $|S_{22}|$  for the optimized T-junction in Fig. 1 (b), (c) and (d). It is noticed that the T-junction in Fig. 1(d) introduced in [3] gives the best response with the least deviation from the ideal value of  $|S_{11}|$  and  $|S_{22}|$ . The response of the T-junction in Fig. 1 (c) introduced here gives slightly better response than the T-junction in Fig. 1 (b) which was introduced in [2].

#### IV. CONCLUSIONS

In this report, we presented a comparison between four configurations for compensating discontinuities in T-junctions. Three of these configurations were mentioned in literature and one is proposed here. The T-junctions are optimized with respect to proper dimensions to satisfy minimum mismatch at the three ports. An accurate 2D EM simulator and a robust optimizer have been utilized to

perform direct optimization. The results of optimization indicates that one of these T-junctions, the one with the removed triangular portion, gives unsatisfactory results and the other give fairly good results with minor differences among their responses

#### REFERENCES

- [1] R. Chadha and K.C. Gupta, "Compensation of discontinuities in planar transmission lines," *IEEE Trans. Microwave Theory Tech.*, vol. 30, 1982, pp. 2151–2156.
- [2] S. Wu, H. Yang and N.G. Alexopoulos, "A rigorous dispersive characterization of microstrip cross and tee junctions," *IEEE MTT-S Int. Microwave Symposium Digest*, 1990, pp. 1151–1154.
- [3] M. Dydyk, "Master the T-junction and sharpen your MIC designs," *Microwaves*, 1977, pp. 184–186.
- [4] D.G. Swanson, Jr., "EM field simulators made practical," Field-Solver Course, M/A-COM Division of AMP Lowell, MA, 1998.
- [5] *em*<sup>TM</sup> Version 4.0b, Sonnet Software, Inc., 1020 Seventh North Street, Suite 210, Liverpool, NY 13088, 1997.
- [6] *OSA90/hope*<sup>TM</sup> and *Empipe*<sup>TM</sup> Version 4.0, formerly Optimization Systems Associates Inc., P.O. Box 8083, Dundas, Ontario, Canada L9H 5E7, now HP EEsof Division, Hewlett-Packard Company, 1400 Fountaingrove, Parkway, Santa Rosa, CA 95403-1799.

TABLE I  
 THE OPTIMAL VALUES OF  $r$  AT  $q$  EQUAL TO  $30^\circ$ ,  $45^\circ$   
 AND  $60^\circ$  FOR THE T-JUNCTION IN FIG. 1(a)

$q$	The optimal value of $r$
$30^\circ$	$1.556 w$
$45^\circ$	$1.355 w$
$60^\circ$	$1.158 w$

TABLE II  
 THE OPTIMAL VALUES OF THE PARAMETERS  $x$  AND  
 $y$  FOR THE T-JUNCTIONS IN FIG. 1(b), (c) AND (d)

T-junction	Optimal value of $x$	Optimal value of $y$
T-junction in Fig. 1(b)	$0.9250 w$	$0.583 w$
T-junction in Fig. 1(c)	$0.7271 w$	$0.7917 w$
T-junction in Fig. 1(d)	$0.1 w$	$0.9167 w$

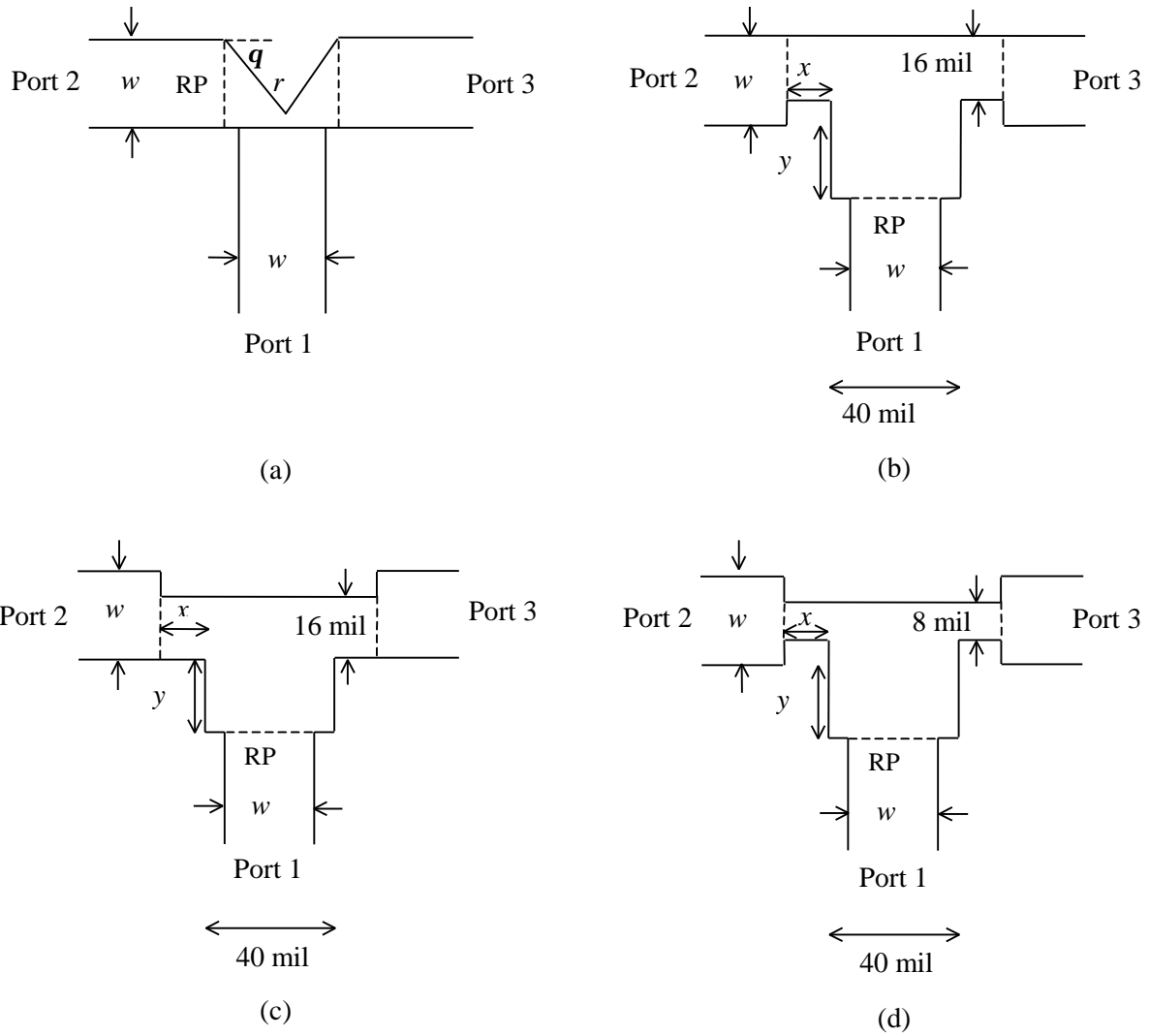


Fig. 1 Four different T-Junction configurations ( $w=24$  mil,  $h=25$  mil and  $\epsilon_r=9.9$ ).

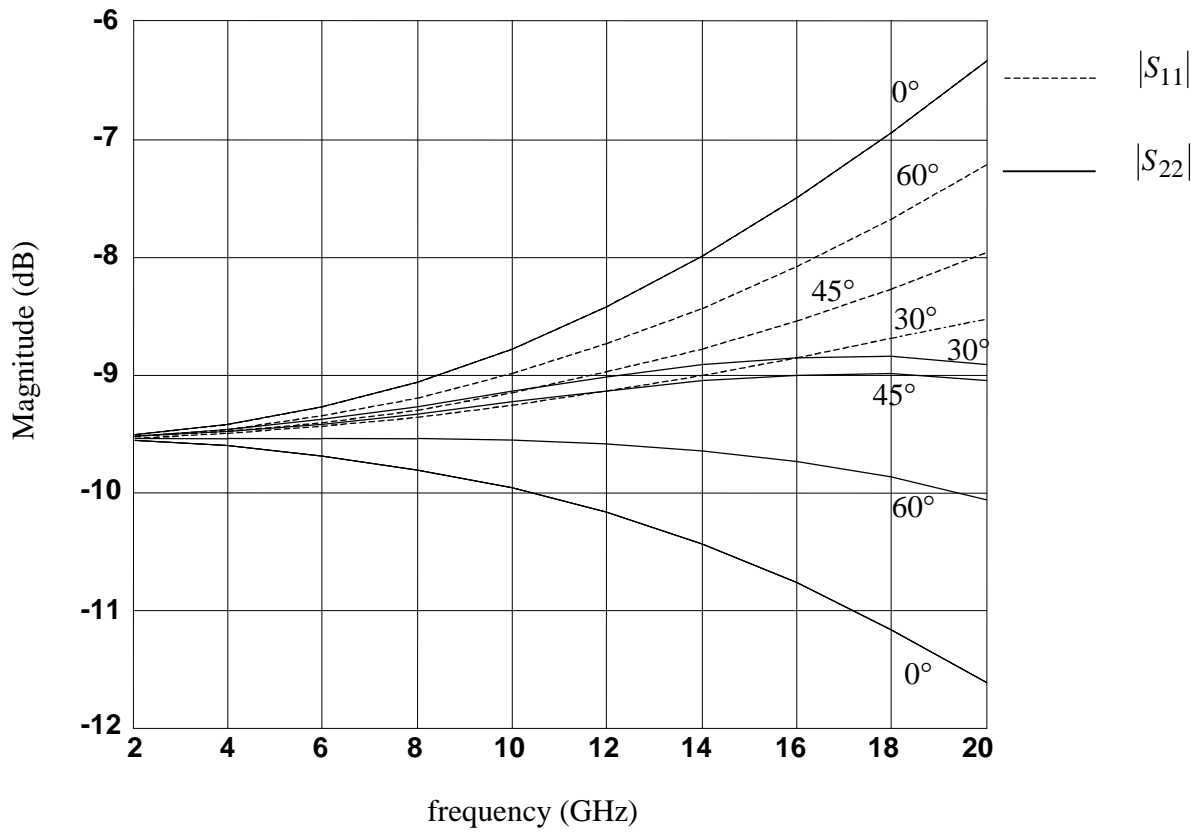


Fig. 2.  $|S_{11}|$  and  $|S_{22}|$  for the T-junction in Fig.1(a) with  $q$  equal to 0, 30°, 45° and 60°.

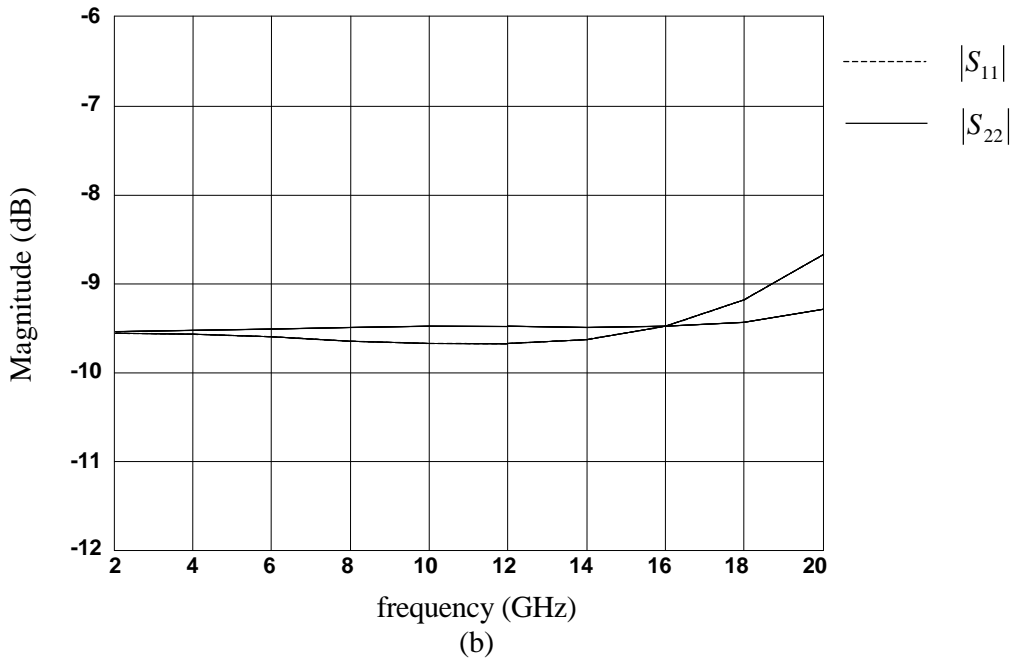
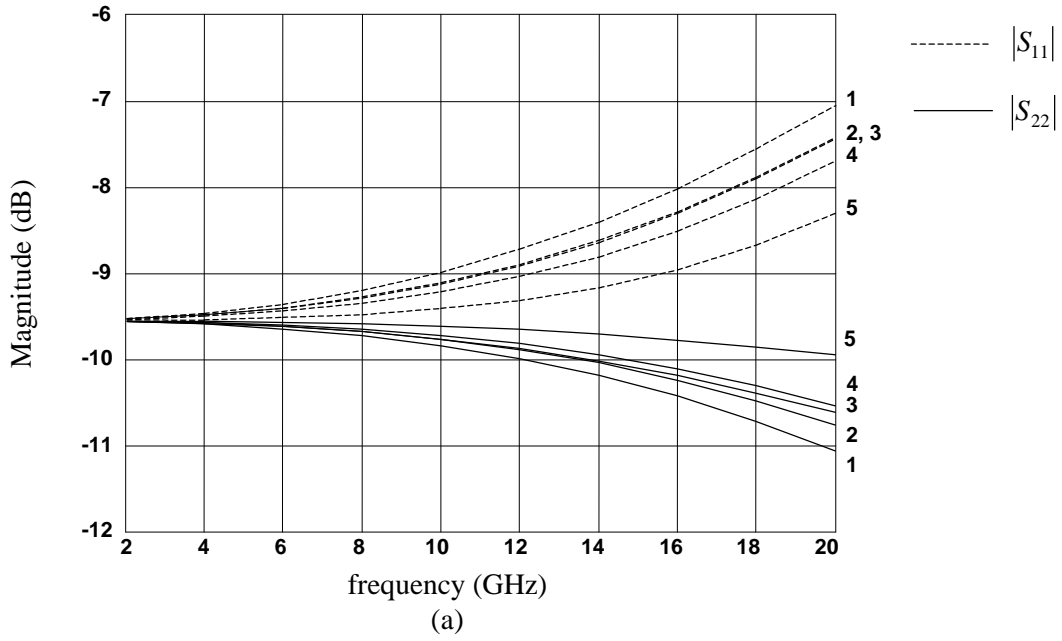


Fig. 3.  $|S_{11}|$  and  $|S_{22}|$  for the T-junction shown in Fig.1(b) before optimization (a) and after optimization (b).

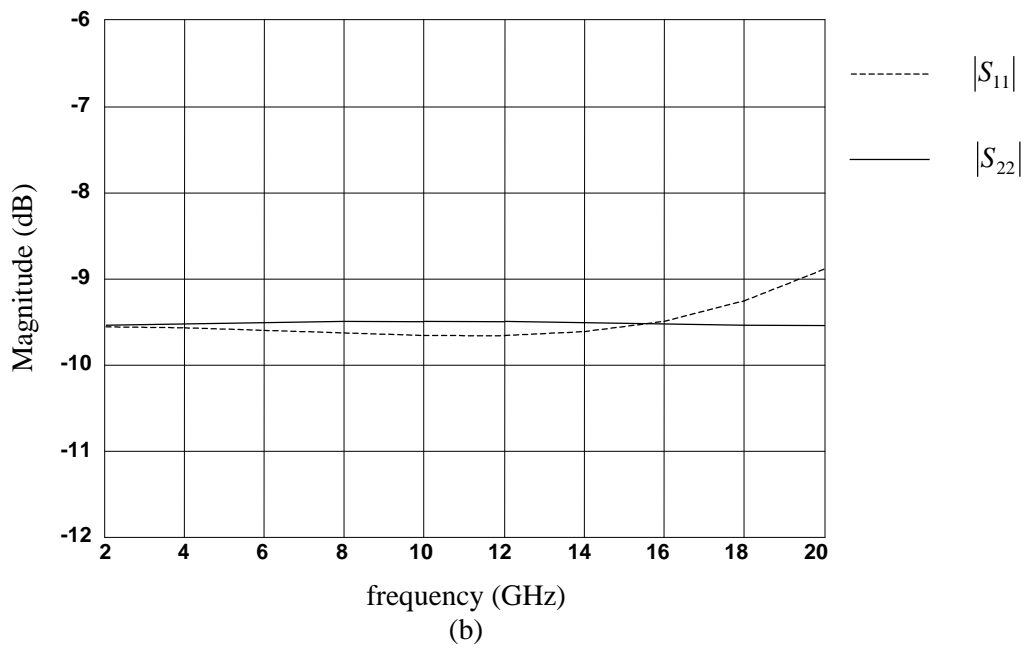
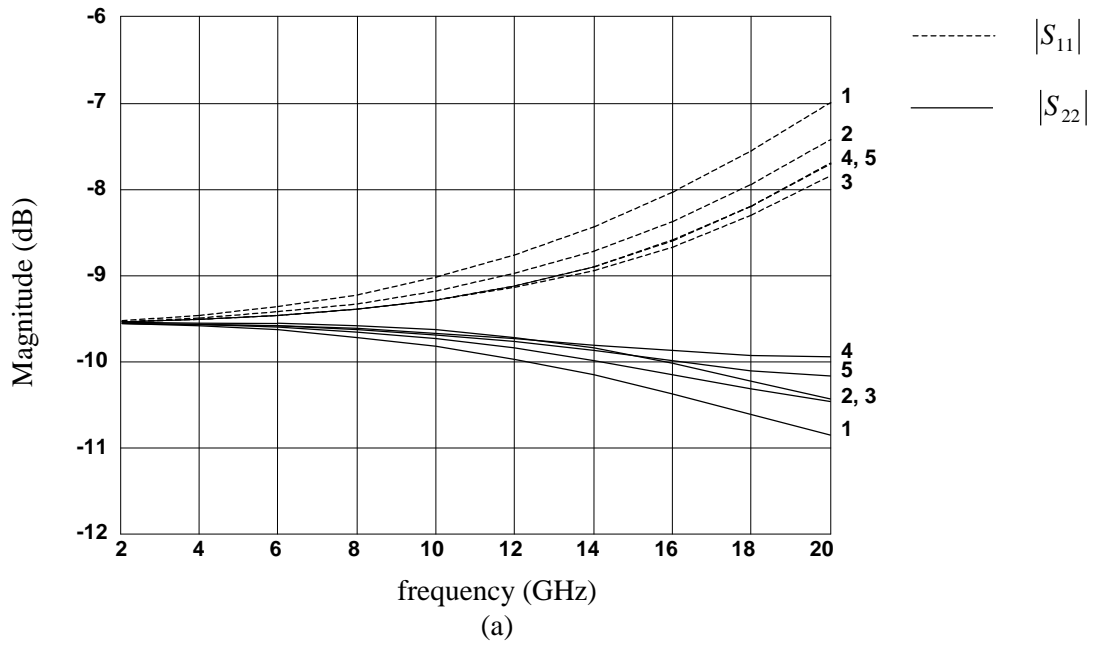


Fig. 4.  $|S_{11}|$  and  $|S_{22}|$  for the T-junction shown in Fig.1(c) before optimization (a) and after optimization (b).

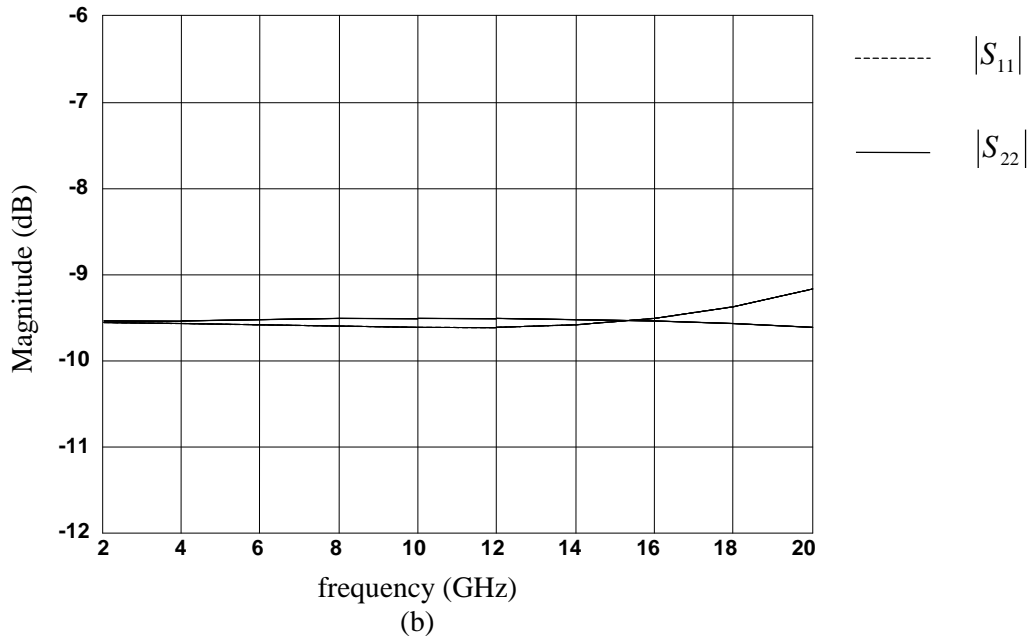
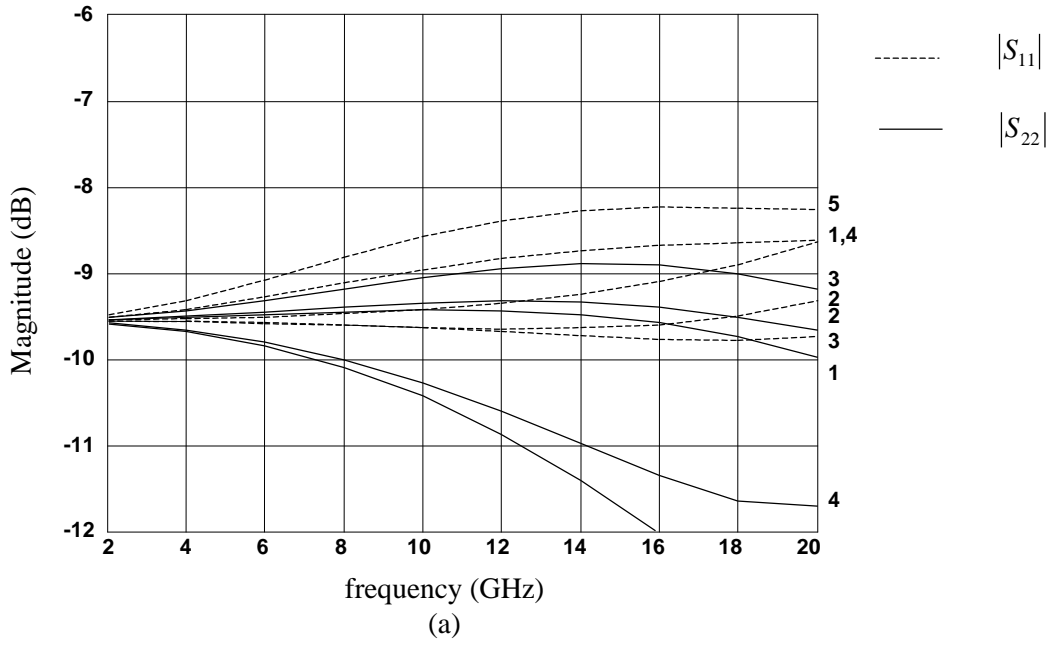


Fig. 5  $|S_{11}|$  and  $|S_{22}|$  for the T-junction shown in Fig.1(d) before optimization (a) and after optimization (b).

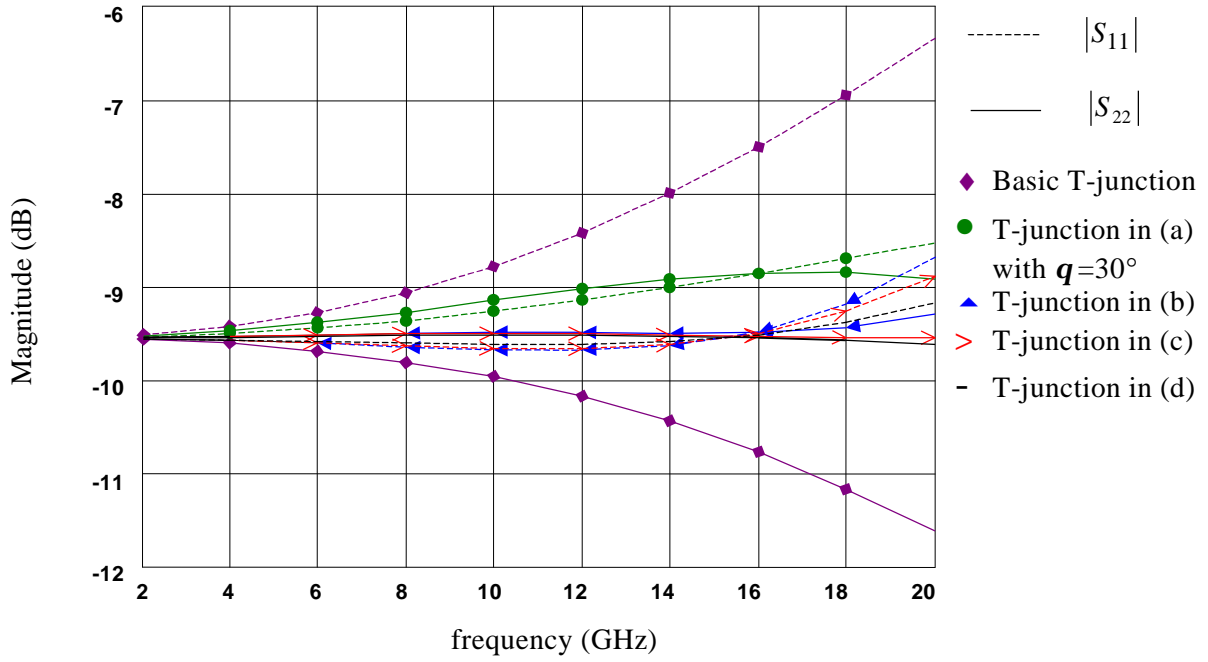


Fig. 6  $|S_{11}|$  and  $|S_{22}|$  for the basic T-junction and the optimized T-junctions shown in Fig.1 (a), (b), (c) and (d).

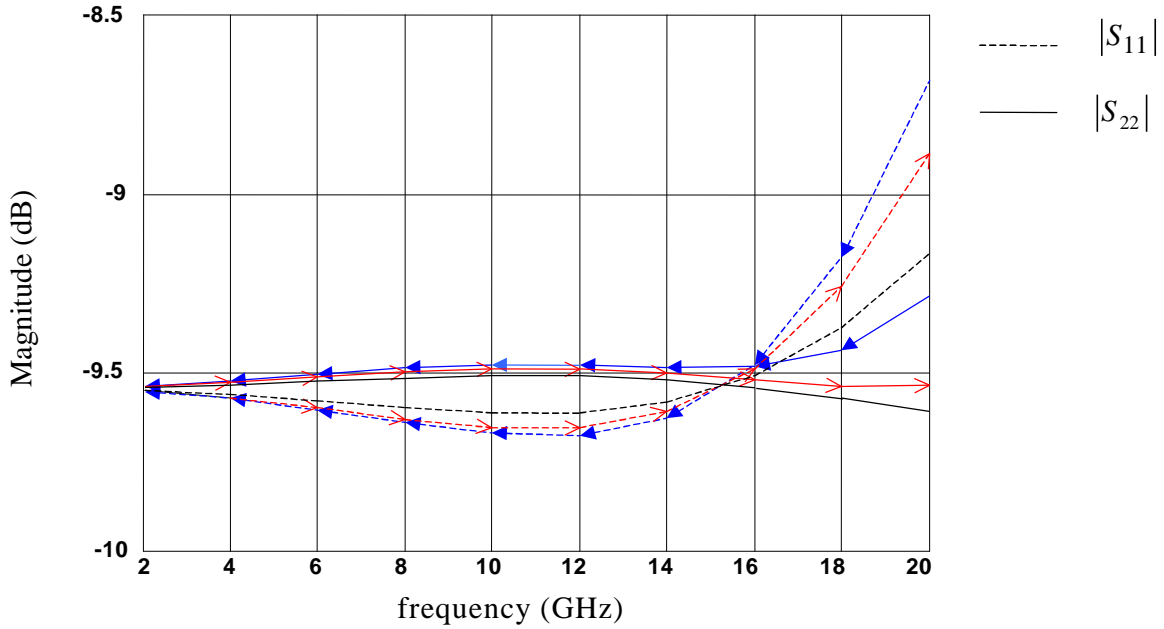


Fig. 7.  $|S_{11}|$  and  $|S_{22}|$  for the optimized T-junctions shown in Fig.1 (b), (c) and (d).